J Solid State Eletrochem (2004) 8: 511–519
DOI 10.1007/s10008-003-0480-y

ORIGINAL PAPER

Fernando Wypych · Michelle S. Meruvia
Luciana B. Adad

Electrochemical intercalation of hydrated cations derived from primary amines into 2H-NbS_2

Received: 15 June 2003 / Accepted: 27 October 2003 / Published online: 24 January 2004

Abstract We report the electrochemical intercalation of three cations derived from amines with different chain length, into the layered compound 2H-NbS_2. The intercalation processes were accompanied by ex situ and in situ X-ray diffraction. For in situ analysis, an electrochemical cell was designed for the purpose. The X-ray diffraction experiments show that the intercalation is a complex process, which involves stacking faults and the formation of stages. When the cations are removed, no changes in the final interplanar basal distances occur, suggesting that there are ideal concentrations of intercalated ions that stabilize the phases. Also, based on the X-ray diffraction results we propose a steric arrangement for the hydrated cations into the van der Waals gaps.

Keywords 2H-NbS_2 · Electrochemical intercalation

Introduction

Intercalation reactions in transition metal dichalcogenides with layered structures are widely described in the literature [1, 2, 3, 4], having their maximum development in the 1970s and 1980s. These studies and the investigation of the superconducting properties of these systems at low temperature, mainly after intercalation reactions [5, 6, 7], suggest intercalation as one of the reasons for the discovery of superconducting ceramic layered systems, towards the end of the 1980s. [8]

F. Wypych (✉) · L. B. Adad
Centro de Pesquisas em Química Aplicada, CEPESQ,
Departamento de Química, Universidade Federal do Paraná,
CP 19081, 81531-990 Curitiba, Pr, Brazil
E-mail: wypych@quimica.ufpr.br
Tel.: 0055-41-361-3297
Fax: 0055-41-361-3186

M. S. Meruvia
Departamento de Física, Universidade Federal do Paraná,
CP 19044, 81531-990 Curitiba, Pr, Brazil

Intercalation processes are very interesting because changes occur in the physical properties of the matrices after intercalation. Also, they can be used in a variety of industrial applications [9], the main ones being related to energy storage in solid-state reversible batteries [10, 11]. Moreover, by exfoliation it is possible to obtain nanocomposites [12, 13, 14, 15] and interesting structures known as "inorganic fullerene-like structures" (IFLS) [16, 17, 18, 19, 20, 21]. The latter occur in a variety of forms such as tubes and spheres with interesting physical properties and with potential tribological applications, under conditions in which liquid lubricants cannot be used [22, 23].

However, despite of the great deal of work done on this subject, the intercalation mechanisms, which involve reduction of the metal in the layers and intercalation of solvated/anhydrous cations, were not completely understood until recently. One of the biggest enigmas involved is the formation of intermediates, which are usually unstable and cannot be indexed, in a single structure. Usually in this process, indexable phases are obtained, where some interlayer gaps are intercalated and others are left completely empty (formation of stages). Only recently some studies of intercalation of hydrated alkaline metal cations in a 2H-NbS_2 layered matrix were reported in the literature [24, 25, 26]. These studies concentrated on electrochemical intercalation reactions followed by in situ X-ray diffraction and on the modeling of the formation of stages and stacking faults during the development of the stable intercalation compounds.

Niobium disulfide occurs in two polymorphs, 3R and 2H [27]. The first one presents a rhombohedral structure, where the repetition of units occurs once every three layers, and the second, hexagonal, where the repetition of units occurs once every two layers. Figure 1 shows the 2H-NbS_2 structure, where the niobium atoms (full circles) are coordinated to six sulfur atoms (open circles) in a trigonal prismatic coordination. The units are bonded to each other by their corners giving rise to layers, which are stacked along the basal direction and separated by

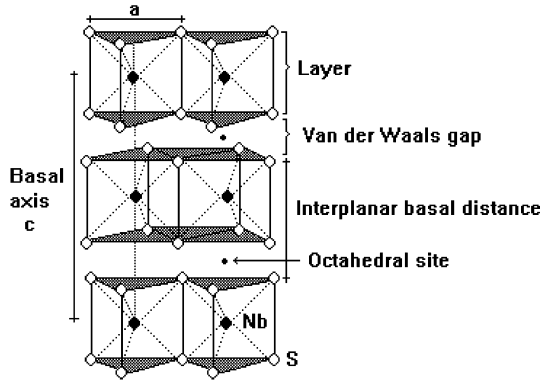

Fig. 1 2H-NbS_2 structure where the open circles correspond to sulfur atoms and the closed ones to niobium atoms

the van der Waals gaps. The atoms in the layer are covalently bonded and layers are held together through van der Waals interactions. These weak forces favor sliding of the individual layers, imparting to this class of compounds their known tribological and intercalation properties. In the van der Waals gaps, the intercalated hydrated ions occupy octahedral sites, which can be described as a set of two tetrahedral sites, in the case of intercalated ions that prefer this geometry. The structure and its units are described in Fig. 1.

The present work presents results obtained from the intercalation of cations derived from hydrated amines into 2H-NbS_2, accompanied by in situ and ex situ X-ray diffraction. In the ex situ mode [28] the samples were obtained by electrochemical reduction using cyclic voltammetry and then scraped from the electrode and in the in situ mode the samples were measured during variation of the electrochemical potential by cyclic voltammetry.

Experimental

The ex situ experiments were performed in a traditional three-compartment electrochemical cell. The reference electrode was a hydrogen electrode, renewed every 12 h and the counter and working electrode were platinum plates of 1 cm^2. A small amount of material in powder form (2–5 mg) was glued in the working electrode with graphite conductive cement (Leit-C—conductive carbon cement, Neubauer Chemikalien, Germany). The electrochemical cell was filled with approximately 30 ml of 0.5 mol/l amine salt solution to be intercalated (methylaminium chloride, propylaminium chloride and hexylaminium sulfate) and the cell coupled to a PARC 273A potentiostat/galvanostat. The scan speed was fixed at 0.5 mV/s. For the X-ray diffraction experiments, the electrode was first polarized for 1 h at the desired potential and subsequently washed with distilled water. The material was removed and mixed with a small amount of silicon powder, which was used as internal standard and then transferred to a glass sample holder.

The reactions involved are described by the following equations:

Reduction reactions:

$$\text{Working electrode}: NbS_2 + xe^- + xA^+ \rightarrow A_x(H_2O)_yNbS_2$$
$$\text{Counter electrode}: H_2O - xe^- \rightarrow xH^+ + \tfrac{x}{2}O_2$$

Oxidation reactions:

$$\text{Working electrode}: A_x(H_2O)_yNbS_2 \rightarrow NbS_2 + xe^- + xA^+$$
$$\text{Counter electrode}: H_2O + xe^- \rightarrow xOH^- + \tfrac{x}{2}H_2$$

For the in situ X-ray diffraction, an electrochemical cell adapted from [29] was built for the purpose and its components are identified and described in the Fig. 2 [30].

In the in situ experiments, a small amount of sample powder was glued with the conductive carbon cement on top of the circular gold working electrode of 1 cm diameter. The reference and counter electrodes were 0.1 mm thick platinum wire and the counter electrode surrounded the working electrode to minimize charge concentration in any particular region in the electrode. Between the Kapton window and the working electrode surface, a 0.6 mm thick solution film was formed. This solution film covering the working electrode surface must be as thin as possible in order to minimize the background noise in the X-ray diffraction measurements. This introduces another problem, namely the low concentration of cations to be intercalated in the vicinity of the sample. To overcome this problem, the concentration of the amine salt solution was increased to 1 mol/l, twice the value for the ex situ experiments. This can be done because upon intercalation, the variation of

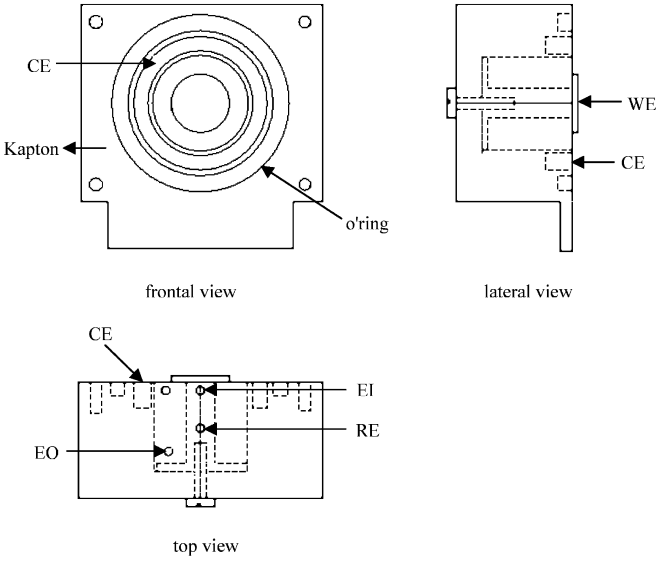

Fig. 2 Electrochemical cell for in situ X-ray diffraction. The cell's components are identified as follows: Teflon body; a Kapton window approximately 10 μm thick; CE, Pt counter electrode; WE, Au working electrode; RE, Pt reference electrode; EO, electrolyte output; EI, electrolyte input. Adapted from [29]

interlayer spacings of layered chalcogenides is independent of electrolyte concentration [31]. To avoid charge concentration gradients, a Milan BP200 peristaltic pump was used with a 0.5 ml/min flux. In the X-ray diffraction measurements the 2θ angle was scanned from 3° to 39° at a sweep rate of 1°/min and the conductive carbon cement used to glue the sample was used as internal standard. Immediately after one scan was obtained the next scan was started, and this process was repeated successively during the reduction and the oxidation processes.

Results and discussion

The cyclic voltammograms of the intercalation/deintercalation of methylaminium ions are shown in Fig. 3. The cycle presents two reduction peaks, at 0.28 V (a) 0.24 V (b), and three oxidation peaks, at 0.34 V (c), 0.38 V (d) and 0.43 V (e).

The X-ray diffraction patterns obtained ex situ and in situ are shown in Figs. 4 and 5, respectively. In both experiments it is possible to observe that the final phase is obtained after formation of intermediates during the intercalation process (Fig. 4a, b and Fig. 5—reduction). These intermediates produce satellite reflections to the right and left of the first characteristic 2H-NbS_2 (002) reflection and, as observed for the intercalation of hydrated cesium and potassium into 2H-NbS_2, they migrate in order to form the (002) and (004) reflections of the new intercalation compound. These reflections cannot be indexed and consist of stages and stacking faults formed during the insertion of cations and their removal from the interlayer spaces [24, 25, 26]. The resulting compound presents an interplanar basal distance of 9.3 Å obtained from Fig. 4c and the last X-ray diffraction pattern of Fig. 5 (reduction). The final phase with

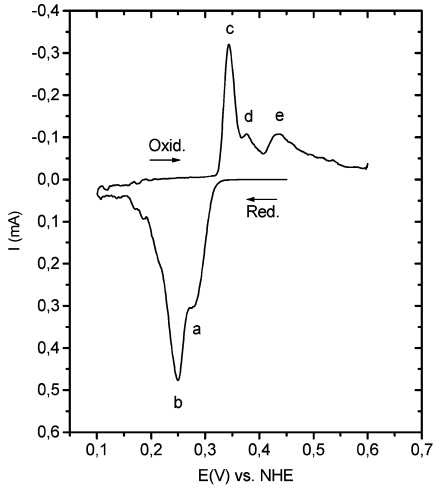

Fig. 3 Cyclic voltammogram for the intercalation of hydrated methylaminium cations into 2H-NbS_2.The arrows indicate the direction of the reaction

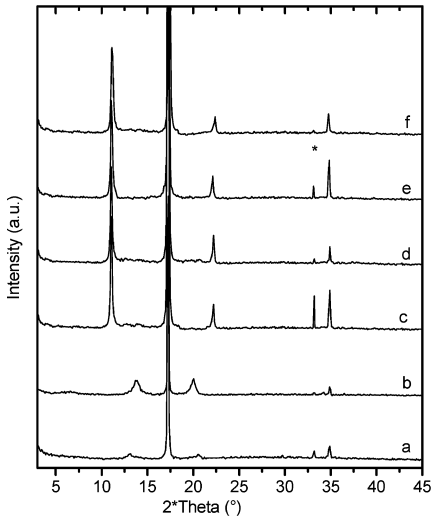

Fig. 4 X-ray diffraction patterns of the methylaminium cations with 2H-NbS_2 reaction products obtained ex situ at different potentials. **a** beginning of the reduction; **b** polarized at 0.24 V; **c** polarized at 0.28 V; **d** polarized at 0.35 V; **e** polarized at 0.38 V; **f** = polarized at 0.43 V

an interplanar distance variation of 3.4 Å corresponds to the hydrated methylaminium cation intercalated in the interlayer spaces. That can be deduced knowing that the diameter of the water molecule is 2.8 Å [31] and the methylaminium cation diameter is 3.34 Å [32]. Also for both experiments, the presence of the initial phase during the whole process was observed, indicating that not all crystals were electrically connected to the electrode. The peaks observed during the oxidation process in the cyclic voltammogram (Fig. 3) indicate a partial reversibility but analyzing Fig. 4d–f, which correspond to deintercalation in different oxidation potentials, there is no evidence of changes in the basal interplanar distance. The in situ observations are in agreement (Fig. 5—oxidation) except for the decrease in intensity of the (002) reflection of the final phase and the disappearance of the (004) reflection after polarization in an oxidant potential. The intensity loss means that fewer planes are diffracting in the same direction, and the oxidation peaks in the voltammogram of Fig. 3 are interpreted as due to decreases in the concentration of intercalated cations. It is reasonable to infer that some layers were completely emptied giving rise to stages in the materials. The same cannot be concluded from the ex situ experiments because for each measurement, a new sample has to be synthesized and variations in intensity can be attributed to differences in sample amounts. The second, third and fourth X-ray diffraction patterns of the reduction process (Fig. 5) are from a different set of measurement and were inserted to show the formation of intermediate phases.

The concentrations of the intercalated species could not be determined with the electrochemical experiment because it was difficult to quantify the amount of the weighed matrix that is immersed in the conductive glue.

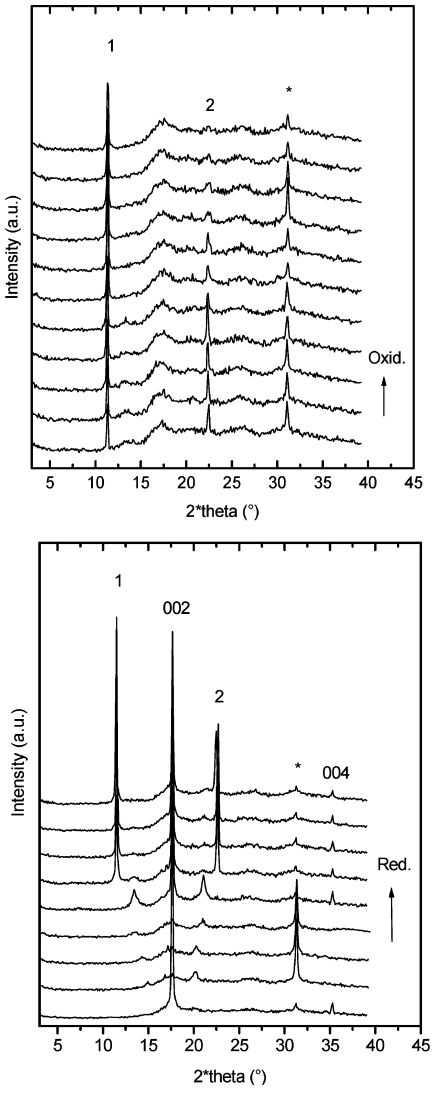

Fig. 5 X-ray diffraction pattern sequences of the electrochemical intercalation (**a**) and de-intercalation (**b**) of the methylaminium cations in 2H-NbS_2 obtained in situ. The reflections indicated by asterisks (*) are from the conductive carbon cement used as internal standard. Only the reflections of 2H-NbS_2 and the phases of the last X-ray diffraction pattern can be indexed by integral indices (*hkl*)

Table 1 Identification of all phases detected in the X-ray diffraction patterns of Fig. 4. The phase 2 is the final phase and phase 3 cannot be indexed. The reflections are indexed as the (00*l*) reflection

X-ray diffraction pattern	2θ (°)	*d* (Å)	Indexation and phases
A	13.05	7.87	Phase 3
	17.24	5.98	002—2H-NbS_2
	20.61	5.00	Phase 3
	33.18	3.17	111—Si
	34.86	2.99	004—2H-NbS_2
B	13.77	7.47	Phase 3
	17.26	5.97	002—2H-NbS_2
	19.98	5.16	Phase 3
	33.18	3.14	111—Si
	34.17	3.05	Phase 3
	34.89	2.99	004—2H-NbS_2
C	11.08	9.29	002—Phase 2
	17.25	5.97	002—2H-NbS_2
	22.16	4.66	004—Phase 2
	33.18	3.14	111—Si
	34.86	2.99	004—2H-NbS_2
D	11.06	9.29	002—Phase 2
	17.25	5.97	002—2H-NbS_2
	22.16	4.66	004—Phase 2
	33.17	3.14	111—Si
	34.88	2.99	004—2H-NbS_2
E	11.06	9.29	002—Phase 2
	17.25	5.97	002—2H-NbS_2
	22.16	4.66	004—Phase 2
	33.17	3.14	111—Si
	34.90	2.98	004—2H-NbS_2
F	11.10	9.26	002—Phase 2
	17.27	5.96	002—2H-NbS_2
	22.20	4.65	004—Phase 2
	33.17	3.14	111—Si
	34.90	2.98	004—2H-NbS_2

Table 2 Data collected during the reduction process of the methylaminium cation intercalation into the 2H-NbS_2 matrix (according to Fig. 5a). The reflections are indexed as the (00*l*) reflection

2θ (°)	*d* (Å)	Δd (Å)
17.33	5.94	–
14.42	7.13	1.19
13.73	7.49	1.55
13.13	7.83	1.89
13.03	7.89	1.95
11.22	9.15	3.21
11.10	9.25	3.31
11.10	9.25	3.31
11.10	9.25	3.31

Tables 1 and 2 present the data obtained using the ex situ and in situ methods, respectively, for intercalation of the methylaminium cation into the 2H-NbS_2 matrix.

Figure 6 shows the cyclic voltammogram for the intercalation of propylaminium cations into 2H-NbS_2. As can be seen, only one large reduction peak centered at 0.14 V (a) is observed with three oxidation peaks at 0.3 V (b), 0.34 V (c) and 0.39 V (d).

Figure 7 shows the X-ray diffraction patterns obtained after scraping the sample from the electrode at determined potentials, which coincide with the reduction and oxidation peaks potentials and are marked by letters from b to e. The X-ray diffraction pattern a corresponds to the first measurement made with samples removed from the electrolyte before the first reduction peak occurred and the one marked with f, is the characteristic (002) 2H-NbS_2 reflection.

As observed for intercalation of methylaminium cations, the intercalation of propylaminium cations occurs with the formation of intermediate steps as can be seen in Fig. 7. The intermediate steps are followed by the formation of the final phase with an interplanar basal distance of 9.6 Å (Fig. 7b). The interplanar distance variation of 3.7 Å corresponds to intercalation of the hydrated propylaminium cation into 2H-NbS_2 van der Waals gaps. This can be deduced knowing that the

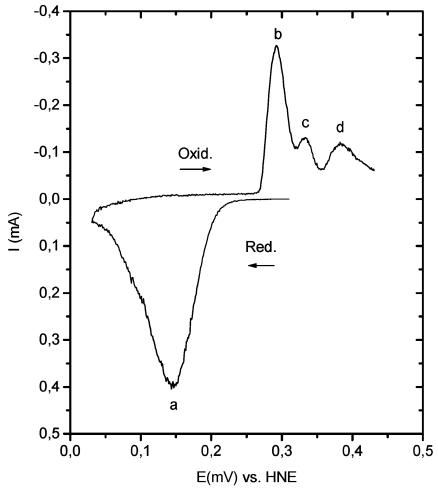

Fig. 6 Cyclic voltammogram for the intercalation of hydrated propylaminium cations into 2H-NbS_2.The arrows indicate the direction of the reaction

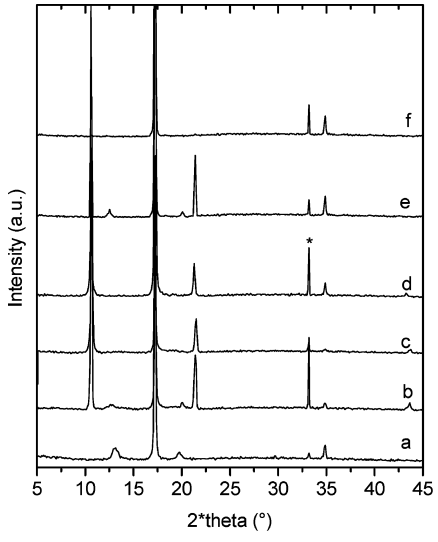

Fig. 7 Sequence of X-ray diffraction patterns obtained ex situ investigation of the reaction products of propylaminium cations with 2H-NbS_2. The reflections indicated by asterisks (*) are from the silicon used as internal standard. **a** beginning of the reduction; **b** polarized at 0.14 V; **c** polarized at 0.3 V; **d** polarized at 0.34 V; **e** polarized at 0.39 V; **f** 2H-NbS_2

diameter of the water molecule is 2.8 Å [31] and that of the propylaminium cation is 3.6 Å [33]. Also, the characteristic (002) reflection of the 2H-NbS_2 appeared in all the X-ray diffraction patterns. The non-regeneration of the matrix indicates that the intercalation process is partially reversible with no modification of the final interplanar basal distance. The phases that were detected in all X-ray diffraction patterns of Fig. 7 are shown in Table 3.

Figure 8 shows the X-ray diffraction patterns obtained during in situ intercalation/de-intercalation of propylaminium cations. In this figure the intermediates

Table 3 Identification of the phases detected in the X-ray diffraction patterns of Fig. 7. Phase 2 is the final phase and phase 3 cannot be indexed

X-ray diffraction pattern	2θ (°)	d (Å)	Indexation and phases
A	13.04	7.88	Phase 3
	17.31	5.96	002—2H-NbS_2
	19.90	5.21	Phase 3
	33.17	3.14	111—Si
	34.90	2.98	004—2H-NbS_2
B	10.64	9.68	002—Phase 2
	17.32	5.96	002—2H-NbS_2
	21.28	4.85	004—Phase 2
	33.13	3.14	111—Si
	34.92	2.98	004—2H-NbS_2
C	10.61	9.55	002—Phase 2
	17.26	5.96	002—2H-NbS_2
	21.32	4.84	004—Phase 2
	33.18	3.14	111—Si
D	10.67	9.63	002—Phase 2
	17.28	5.96	002—2H-NbS_2
	21.47	4.81	004—Phase 2
	33.18	3.14	111—Si
	34.95	2.98	004—2H-NbS_2
E	10.62	9.58	002—Phase 2
	12.51	8.21	Phase 3
	17.21	5.98	002—2H-NbS_2
	20.06	5.14	Phase 3
	21.37	4.83	004—Phase 2
	33.18	3.14	111—Si
	34.82	2.99	004—2H-NbS_2
F	17.28	5.96	002—2H-NbS_2
	33.18	3.14	111—Si
	34.99	2.98	004—2H-NbS_2

formed during the reduction process and its evolution to the final phase are more visible. The resulting interplanar basal distance is 9.6 Å. After oxidation c-axis contraction of the final phase did not occur, but again the decrease in intensity of reflections associated with the oxidation peaks can be interpreted, as previously discussed, as due to a partial reversibility of the system. Table 4 shows the values of the reflections position in the X-ray diffraction patterns (2θ), interplanar distance (d in Å) and interplanar expansions (Δd in Å) obtained for the reduction process.

The cyclic voltammogram of the hexylaminium cation intercalation and de-intercalation processes are shown in Fig. 9. In the cycle, there are three reduction peaks at 0.08 V (a), 0.05 V (b) and 0.01 V (c) and only one oxidation peak at 0.08 V (d).

For the ex situ analysis the same procedure as described previously was followed. The samples were taken out of the cell after polarization at previously determined potentials indicated in the cyclic voltammograms and then taken to the diffractometer (Fig. 10).

Analyzing the first X-ray diffraction pattern (Fig. 10a), it is possible to see that the intercalation reaction occurs with the formation of a major product, which presents an interplanar basal distance of 9.9 Å, which corresponds to an interplanar expansion of 4 Å. The hexylaminium cation chain diameter is approxi-

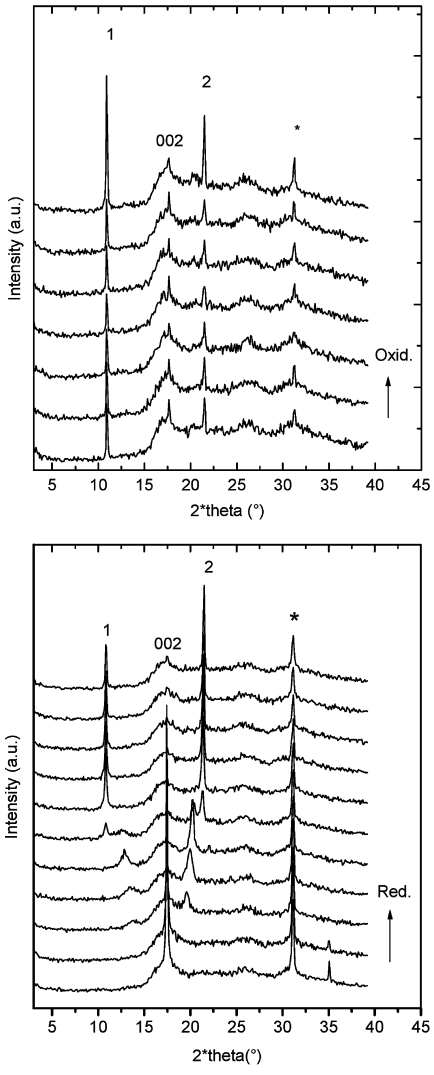

Fig. 8 Sequences of X-ray diffraction patterns obtained in situ for the intercalation (**a**) and de-intercalation (**b**) of propylaminium cations in 2H-NbS_2

Table 4 Data obtained during the reduction process for the intercalation of the propylaminium cation into the 2H-NbS_2 matrix (according to Fig. 8a). The reflections are indexed as the (00 l) reflection

2θ (°)	d (Å)	Δd (Å)
17.33	5.94	–
17.33	5.94	–
13.72	7.49	1.55
13.3	7.73	1.79
12.71	8.09	2.15
12.47	8.24	2.3
10.69	9.6	3.66
10.69	9.6	3.66
10.69	9.6	3.66

mately 4 Å [28], this expansion being attributed to the intercalated cations of carbon chain arranged parallel to the disulfide layers. This first phase is followed by second (Fig. 10b) and third (Fig. 10c) phases with interplanar

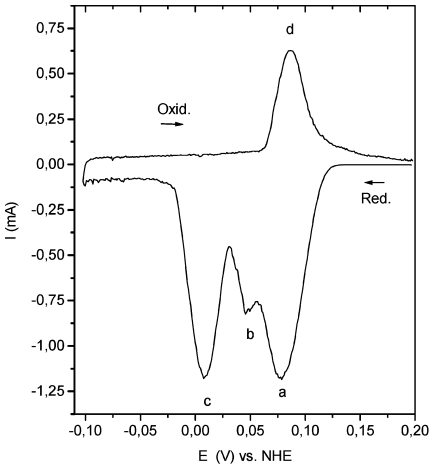

Fig. 9 Cyclic voltammogram for the intercalation of the hexylaminium cation into 2H-NbS_2. The arrows indicate the direction of the process

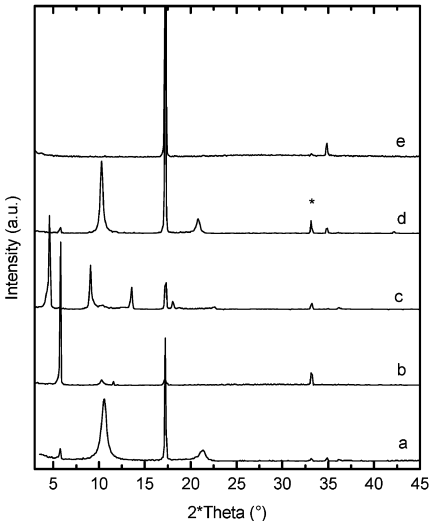

Fig. 10 Ex-situ X-ray diffraction patterns of the 2H-NbS_2 reaction products with hexylaminium cations. The reflections indicated by asterisks (*) are from the silicon used as internal standard. **a** polarized at 0.08 V; **b** = polarized at 0.05 V; **c** polarized at 0.01 V; **d** polarized at 0.08 V; **e** = NbS_2

basal spacings of 17.7 Å and 22.9 Å, respectively. The second phase presents a variation in layer separation of 11.8 Å. As the hexylaminium cation has a chain length of 8.8 Å [34, 35], the expansion observed for this case is 3 Å, larger than expected, compatible with the addition of a water monolayer coordinated to the hexylaminium cations, arranged perpendicularly to the disulfide layers. The hydrated chains turned alternately up and down with the amine group adjacent to the sulfur atoms. With the increasing Nb^{+3} concentration, more cations need to be inserted to balance the negative charge in the layer, and this gives rise to the third phase with a variation in interplanar basal distance of 17 Å. The perpendicular arrangement of a double layer of hydrated ions would

Table 5 Identification of all phases detected in the X-ray diffraction patterns of Fig. 10. Phase 1, 17.7 Å; phase 2, 9.9 Å; phase 3, 22.9Å

X-ray diffraction pattern	2θ (°)	d (Å)	Indexation and phases
A	5.76	17.8	002—Phase 1
	10.56	9.73	002—Phase 2
	17.22	5.98	002—2H-NbS_2
	21.32	4.84	004—Phase 2
	33.13	3.14	111—Si
	34.84	2.99	004—2H-NbS_2
B	5.80	17.7	002—Phase 1
	10.29	9.98	002—Phase 2
	11.57	8.88	004—Phase 1
	17.19	5.99	002—2H-NbS_2
	17.45	5.90	006—phase 1; 002—2H-NbS_2
	33.13	3.14	111—Si
C	4.48	22.90	002—Phase 3
	9.00	11.41	004—Phase 3
	10.24	10.03	002—Phase 2
	13.47	7.63	006—Phase 3
	17.19	5.99	002—2H-NbS_2
	18.01	5.72	008—Phase 3
	22.49	4.59	0010—Phase 3
	33.13	3.14	111—Si
	36.09	2.89	0016—Phase 3
D	5.77	17.80	002—Phase 1
	10.28	9.99	002—Phase 2
	17.82	5.78	008—Phase 3
	20.84	4.95	004—Phase 2
	33.13	3.14	111—Si
	34.84	2.99	004—2H-NbS_2
	42.14	2.49	008—Phase 2

give an expansion of 20.6 Å, higher than that observed, but considering the rigidity of the cations chains, the only possible arrangement for the molecules is a double layer with a tilt angle of 55° with the disulfide layers. This arrangement has already been proposed for *n*-alkylamines intercalated in TaS_2 [36] and is an interesting arrangement since these systems are used for removal of nonpolar solvents through ad-solubilization, when the intercalated species act as a solvent to molecules with similar polarity. After the oxidation process, the final phase with an interplanar basal distance of 9.9 Å stabilizes, forming a monolayer with the molecules positioned parallel to the layers. This effect can be easily explained considering that the hexylaminium ions occupy a large volume in the van der Waals gaps, so that when the charge concentration is decreased, the molecules rearrange in order to form the stable phase. As can be seen, the characteristic reflection of the 2H-NbS_2 is present in all the X-ray diffraction patterns. In Table 5 the phases detected in all X-ray diffraction patterns of Fig. 10 are shown.

Figure 11 shows the in situ X-ray diffraction patterns obtained for the intercalation and de-intercalation of hexylaminium cations. Preceding the first phase, characterized by a basal interplanar distance of 9.8 Å, there are intermediate compounds. Also, during the reduction process a mechanism of formation of intermediates is

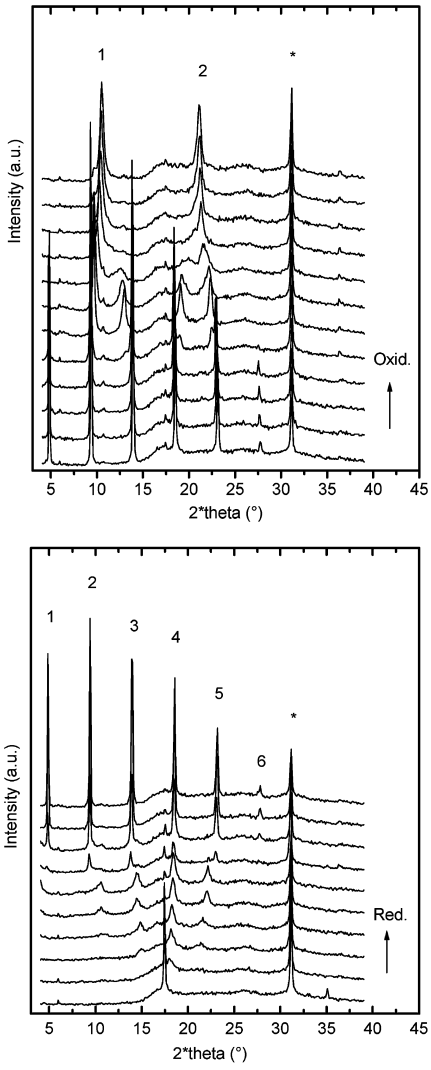

Fig. 11 Sequences of in situ X-ray diffraction patterns obtained for the intercalation (**a**) and de-intercalation (**b**) of the hexylaminium cation

observed and the final phase is reached without observation of the second phase, in which the cation monolayer is arranged perpendicularly between the layers. The final phase obtained presents an interplanar basal distance of 21.7 Å, a value slightly different from the 22.9 Å observed by ex situ X-ray measurements. This value would give an inclination of 50° for the hydrated double layer assuming that there is no superposition of the carbon chains. After the oxidation process has ended, the final phase is the same as that observed in the ex situ measurements, with the cations arranged forming a monolayer parallel to the disulfide layers. This means that the system is reversible for the second and third reduction processes but not for the first one. Table 6 presents the values obtained for the reflections positions in the X-ray diffraction patterns (2θ), for the basal interplanar distances (d) and interplanar expansions (Δd).

Table 6 Data collected for the hexylaminium cation intercalation (reduction) and de-intercalation (oxidation) into the 2H-NbS_2 matrix (according to Fig. 11)

2θ (°) Oxidation	d (Å)	Δd (Å)
Reduction		
17.33	5.94	–
17.33	5.94	–
17.33	5.94	–
14.82	6.94	1
14.82	6.94	1
10.46	9.82	3.88
10.46	9.82	3.88
4.72	21.71	15.77
4.72	21.71	15.77
4.72	21.71	15.77
4.72	21.71	15.77
4.72	21.71	15.77
4.72	21.71	15.77
4.72	21.71	15.77
4.72	21.71	15.77
4.72	21.71	15.77
4.72	21.71	15.77
9.48	10.83	4.89
9.54	10.76	4.82
9.83	10.45	4.51
10.17	10.09	4.15
10.28	9.99	4.05
10.4	9.88	3.94
10.4	9.88	3.94

Conclusions

The intercalation experiments followed by cyclic voltammetry and in situ and ex situ X-ray diffraction measurements allows us to conclude that:

- In the intercalation of methylaminium cation the reduction peaks are related to the formation of stages and phases that cannot be indexed, as well as to the stabilization of the final phase where the cations are intercalated as monolayers. The three oxidation peaks are related to the decrease in concentration of intercalated species through Nb^{+3} oxidation. In this case, the concentration of intercalated species does not interfere with its positioning between the layers and as a consequence the interplanar distance remains unchanged.
- In the intercalation of hydrated propylaminium cations, one large reduction peak and three small oxidation peaks were observed. Similarly, the mechanisms for the formation of intermediates in intercalation of methylaminium cations were observed. In the sequence, the final phase formed with the hydrated propylaminium cations intercalated as a monolayer in the van der Waals gaps.
- Since the hexylaminium cation has a longer chain, the concentration of the species occupying the van der Waals gaps allows different ordering and consequently the observation of different compounds [36]. The first peak in the reduction process is attributed to the formation of a monolayer of hexylaminium cations intercalated in the van der Waals gaps. This phase formed initially, as observed by X-ray diffraction, and corresponds to a phase where the hexylaminium cations intercalate forming a monolayer with the molecules arranged parallel to the layers. As the reduction process proceeds, two new structural configurations are observed; one in which the molecules form a monolayer perpendicular to the layers and the second where the aminium cations form a bilayer, which lies tilted at an angle of 55° to the basal direction. The oxidation process decreases the concentration of the intercalated cations and the final and stable phase achieved is the one in which the cations are arranged forming a monolayer parallel to the disulfide layers.

References

1. Motizuki K, Nishio Y, Shirai M, et al (1996) J Phys Chem Solids 57:1091
2. Evans JSO, Price SJ, Wong HV, O'Hare D (1998) J Am Chem Soc 120:10837
3. O'Hare D, Evans JSO, Price SJ (1998) J Chin Chem Soc 45:591
4. O'Hare D, Evans JSO, Fogg A, O'Brien S (2000) Polyhedron 19:297
5. Chen B, Eichhorn B, Peng J, Greene RL (1993) J Solid State Chem 103:307
6. Molenda J, Bak T, Marzec J (1996) Phys Stat Solidi A 156:159
7. Motizuki K, Nishio Y, Shirai M, Suzuki N (1996) J Phys Chem Solids 57:1091
8. Bednorz JG, Mueller KA (1986) Z Phys B 64:189
9. Wypych F, (2002) Quím Nova 25:83
10. Mulhern P, (1989) Can J Phys 67:1049
11. Hernan L, Morales J, Sanches L, et al (1994) Electrochem Acta 39:2665
12. Divigalpitiya WMR, Frindt RF, Morrison SR (1989) Science 246:369
13. Wypych F, Adad LB, Grothe MC (1998) Quím Nova 21:687
14. Lemaux S, Golub AS, Gressier P, Ouvrard G (1999) J Solid State Chem 147:336
15. Yang D, Westreich P, Frindt RF (1999) Nanostruct Mat. 12:467
16. Feldman Y, Frey GL, Homyonfer M, Lyakhovitskaya V, Margulis L, Cohen H, Hodes G, Hutchison JL, Tenne R (1996) J Am Chem Soc 118:5362
17. Zak A, Feldman Y, Alperovich V, Rosentsveig R, Tenne R (2000) J Am Chem Soc 122:11108
18. Seifert G, Terrones H, Terrones. M, Frauenheim T (2000) Solid State Commun 115:635
19. Zak A, Feldman Y, Lyakhovitskaya V, Leitus G, Popovitz-Biro R, Wachtel E, Cohen H, Reich S, Tenne R (2002) J Am Chem Soc 124:4747
20. Li YD, Li XL, He RR, Zhu J, Deng ZX (2002) J Am Chem Soc 124:1411
21. Tenne R (2002) Colloids Surf A 208:83
22. Rapoport L, Lvovsky M, Lapsker I, Leshchinsky V, Volovik Y, Feldman Y, Margolin A, Rosentsveig R, Tenne R (2001) Nano Lett 1:137
23. Cizaire L, Vacher B, Le Mogn T, Martin JM, Rapoport L, Margolin A, Tenne R (2002) Surf Coat Technol 160:282
24. Paulus W, Katzke H, Schöllhorn R (1992) J Solid State Chem 96:162
25. Katzke A (2002) Z Krystallogr 217:127

26. Katzke A (2002) Z Krystallogr 217:149
27. Rao GVS, Shafer MW (1979) In: Levy F (ed) Intercalated layered materials, vol 6. Reidel, Dordrecht
28. Adad LB (1999) Dissertação de Mestrado, Universidade Federal do Paraná, Brazil
29. Gholamabbas N, Muller RH (1985) J Electrochem Soc 132:1385
30. Meruvia MS (2000) Dissertação de Mestrado, Universidade Federal do Paraná, Brazil
31. Lerf A, Schöllhorn R (1977) Inorg Chem 16:2950
32. Molitor M, Müller-Warmuth W, Spiess HW, Schöllhorn R (1983) Z Naturforsch 38a:237
33. Nazri G, Muller RH (1985) J Electrochem Soc 132
34. Wypych F, Gomes MAB, Denicoló I, Adad LB (1996) J Electrochem Soc 143:2522
35. Wypych F, Gomes MAB, Denicoló I, Adad LB (1997) Quím Nova 20:14
36. Jacobson AL (1982) In: Whittingham MS, Jacobson AJ (eds) Intercalation chemistry, organic and organometallic intercalation compounds of the transition metal dichalcogenides. Academic Press, New York, p 229